Eumitrins C-E: Structurally diverse xanthone dimers from the vietnamese lichen Usnea baileyi

Van-Kieu Nguyen, Grégory Genta-Jouve, Thuc-Huy Duong, Mehdi Beniddir, Jean-François Gallard, Solenn Ferron, Joël Boustie, Elisabeth Mouray, Philippe Grellier, Warinthorn Chavasiri, et al.

Eumitrins C-E: Structurally Diverse Xanthone Dimers From The Lichen *Usnea baileyi*

Van-Kieu Nguyen[a], Grégory Genta-Jouve[b], Thuc-Huy Duong[c] , Mehdi A. Beniddir[d], Jean-François Gallard[e] , Solenn Ferron[f], Joël Boustie[f], Elisabeth Mouray[g], Philippe Grellier[g], Warinthorn Chavasiri[a,□,*] and Pierre Le Pogam[f,□, *]

[a]Center of Excellence in Natural Products Chemistry, Department of Chemistry, Faculty of Science, Chulalongkorn University, Pathumwan, Bangkok 10330, Thailand.
[b]Faculté de Pharmacie de Paris, C-TAC, UMR 8638 CNRS Université Paris Descartes, Sorbonne Paris Cité, 4 Avenue de l'Observatoire, 75006 Paris, France.
[c]Department of Chemistry, Ho Chi Minh city University of Education, Vietnam
[d] Équipe "Pharmacognosie-Chimie des Substances Naturelles", BioCIS, Université Paris-Sud, CNRS, Université Paris-Saclay, 5 Rue J.-B. Clément, 92290 Châtenay-Malabry, France
[e]Institut de Chimie des Substances Naturelles, CNRS, ICSN UPR 2301, Université Paris-Saclay, 1 Avenue de la Terrasse, 91198 Gif-sur-Yvette, France.
[f] Univ Rennes, CNRS, ISCR (Institut des Sciences Chimiques de Rennes) – UMR 6226, F-35000 Rennes, France.
[g]Muséum National d'Histoire Naturelle, Unité Molécules de Communication et Adaptation des Micro-organismes, UMR7245, CP54, 57 Rue Cuvier, 75005, Paris, France.
□ These authors contributed equally to this job.
Email: warinthorn.c@chula.ac.th, pierre.le-pogam-alluard@u-psud.fr

ABSTRACT: Three new xanthone dimers, eumitrins C–E (**1**–**3**), along with a new depsidone, 3'-*O*-demethylcryptostictinolide (**4**) were isolated from the acetone extract of the whole thallus of the lichen *Usnea baileyi* collected in Vietnam. Their structures were unambiguously established by spectroscopic analyses (HRESIMS, 1D and 2D NMR), as well as comparison to literature data.Absolute configurations of **1**–**3** were elucidated through electronic circular dichroism analyses. The absolute configurations of **2** was validated by comparison between experimental and TDDFT-calculated ECD spectra (**2**) while that of **3** was based on DFT-NMR calculations and subsequent DP4 probability score. The antiparasitic activities against *Plasmodium falciparum* as well as the cytotoxic activity against seven cell lines were determined for new compounds **1**–**3**, and led from null to mild bioactivities.

1. Introduction

Lichens are widespread symbiotic systems comprising a fungus and a photosynthetic partner (green algae and/or cyanobacteria). This original lifestyle is associated with a dedicated chemodiversity, so far sustained by *ca.* 1400 specialized metabolites (personal data), a vast majority of which are unique to the lichenized condition.[1] Within this underexplored chemodiversity, a collection of structurally unique xanthones has been reported[2] . Ergochrome dimers related to the eumitrin[3] and secalonic acid series in particular[4, 5] were scarcely isolated from lichen sources, in particular from *Usnea* species. Such dimeric xanthones are privileged structures since they are endowed with various and often significant bioactivities.[6]

Accordingly, secalonic acids exhibit a wide array of bioactivities including cytotoxic, antibacterial, antitumor, and anti-HIV properties.[7] The structurally-related tetrahydroxanthone atropisomer phomoxanthone A from the mangrove-associated fungus *Phomopsis longicolla* also displays promising antitumor properties,[8] renewing the interest in isolating and synthesizing new derivatives from this structural class. Secalonic acids are also of utmost interest since they are reported to occur as mycotoxins with toxic, fetotoxic/teratogenic, and mutagenic

properties.[9] The structure elucidation of such compounds often turns out to be tricky owing to the elevated number of stereochemical centers and symmetries. Indeed, dimeric xanthones reveal varying degrees of barrier to rotation, ranging from freely rotating within microseconds time-frame to isolable and stable atropisomers. Therefore, the absolute stereochemical assignation of regioisomerically similar xanthone dimers is in many case incomplete.[6] Fully addressed stereochemical issues related to dimeric xanthones mostly arose from X-ray structures, (*i. e.* the recently-reported lichen-derived usneaxanthones[10] so that only a few xanthone dimers benefitted from modern time dependent density function theory (TDDFT) calculations of electronic circular dichroism (ECD) spectra to support such outcomes so far.[11, 12] These structure elucidation strategies limit the availability of complete ^{1}H and ^{13}C NMR datasets for xanthone dimers, rendering more difficult the assignment of new compounds from this phytochemical class. The fruticose lichen *Usnea baileyi* (Stirt.) Zahlbr. has been phytochemically investigated by several authors and reported to contain depsides (barbatic and thamnolic acids), depsidones (protocetraric, norstictic, and salazinic acids), aliphatic and paraconic acids (caperatic and protolichesterinic acids), the dibenzofuran-related usnic acid, and xanthone dimers.[3, 13] As to this latter phytochemical group, the late Asahina first reported on the occurrence of yellow pigments within *U. baileyi*, the so-called eumitrins A_1, A_2, B, and T.[14] A few years later, Shibata and co-workers elucidated these eumitrins.[3] The HPLC-based chemical profiling of *Usnea baileyi* recently revealed the occurrence of a wider set of dimeric xanthones, including eumitrins A_3 and B_2, which are still to be structurally elucidated.[15] Some other unidentified dimeric xanthones were also reported from different lichen sources, namely eumitrin U, X and Y.[16-18]

In the search for new xanthone dimers from lichen source, our previous phytochemical investigation of the acetone extract of *U. baileyi* led to the isolation and structure elucidation of bailexanthone, along with a new depsidone, bailesidone.[19] The current study reports the isolation, structure elucidation, and evaluation of antiparasitic and cytotoxic activities of three new xanthone dimers: eumitrin C–E (**1**–**3**), along with a new depsidone, 3'-*O*-demethylcryptostictinolide (**4**). The structure elucidation of these new dimer xanthones benefitted from an extensive array of spectroscopic techniques and stand among the first extensive ^{1}H and ^{13}C NMR complete assignments within the secalonic acid/ergochrome derivatives, that were most often determined based on single-crystal X-ray crystallography analysis.

2. Experimental section

2.1. General Experimental Procedures.

Specific rotations were obtained on a Perkin-Elmer 341 digital polarimeter. Electronic Circular Dichroism and corresponding UV-visible spectra were measured on a Jasco J-815 spectropolarimeter. The IR spectra were acquired using a Shimadzu FTIR-8200 infrared spectrophotometer. 1D and 2D NMR spectra were acquired using a Bruker Advance 400 MHz or a Bruker AM-500 MHz spectrometer. Chemical shifts are referenced to the residual solvent signal ($CDCl_3$: δ_H = 7.26, δ_C = 77.16). HRESIMS data were recorded using a Bruker MicroTOF Q-II mass spectrometer. Open-column chromatography separations were performed on silica gel (40-63 μm, Himedia). TLC analyses were carried out on precoated silica gel 60 F_{254} or silica gel 60 RP-18 F_{254}S plates (Merck), and spots were visualized by spraying with 10% H_2SO_4 solution followed by heating.

2.2. Lichen Material.

Whole thalli of *Usnea baileyi* (Parmeliaceae) were collected from the bark of trees in Tam Bo mountain (elev. 1000 m), Di Linh district, Lam Dong province, Vietnam in 05/2015. The lichen was identified by Dr. Ek Sangvichien

and Ms. Natwida Dangphui. A voucher specimen (UP-014) was deposited in the herbarium of the department of Organic Chemistry, Faculty of Chemistry, Ho Chi Minh University of Education (Vietnam).

2.3. Extraction and Isolation.

The dried thalli of *U. baileyi* (800 g) were crushed and extracted with acetone (4 x 4 L) at room temperature for 24 h. The filtered solution was evaporated to dryness under reduced pressure to obtain a crude acetone extract (80 g). This crude extract was resuspended in acetone to afford an acetone-soluble fraction (ACS, 56.3 g), and a precipitate (ACP, 23.7 g). Fraction ACS was applied to silica gel solid-phase extraction and successively eluted with DCM, EtOAc, acetone, and methanol to afford the corresponding fractions: DCM (31.2 g), EtOAc (9.6 g), acetone (6.5 g), and MeOH (4.6 g). DCM fraction was subjected to silica gel column chromatography using a solvent system of *n*-hexane/EtOAc (8 :2 to 0 :1) to afford four subfractions DCM1-4. Subfraction DCM2 (9.5 g) was selected for further fractionation by normal-phase silica gel column chromatography using an isocratic mobile phase consisting of *n*-hexane/DCM/MeOH (5 :5 :0.1) to afford subfractions DCM2.1-5. Fraction DCM2.2 (1.2 g) was separated by open-air column chromatography using an isocratic elution solvent system consisting of *n*-hexane/EtOAc (6 :4) to afford three fractions DCM2.2.1-3. Further fractionation of DCM2.2.1 (201 mg) by silica gel column chromatography using a *n*-hexane /DCM/EtOAc (3 :2 :1) solvent system to afford compounds **1** (4.6 mg), **2** (3.7 mg), **3** (1.1 mg), and **4** (1.5 mg).

2.4. Biological Assays.

The cytotoxicity of compounds **1**−**3** was evaluated against a panel of 6 representative cell lines, namely Huh7 (differential hepatocellular carcinoma), Caco 2 (differentiating colorectal adenocarcinoma), MDA-MB-231 (breast carcinoma), HCT-116 (actively proliferating colorectal carcinoma), PC-3 (prostate carcinoma), NCI-H2 (lung carcinoma), and diploid skin fibroblasts as normal cell lines for control. Cells were grown as reported elsewhere and the inhibition of cell proliferation was determined as in Coulibaly et al.[20] All tests were conducted in triplicate and the results were averaged. Compounds **1**−**3** were also assayed for their antiparasitic activity against the chloroquine-resistant strain of *Plasmodium falciparum* FcB1. The details of the experimental procedure for this bioassay are similar to those formerly reported.[21]

2.5. Computational Details.

All DFT calculations have been performed using Gaussian 16W.[22] Prior to geometry optimization, all compounds were submitted to a conformational analysis using the GMMX package with the MMFF94 forcefield (energy threshold=1 kcal/mol). After geometry optimization and frequency calculation at the b3lyp/6-31g(d) level. NMR properties were calculated at the mpw1pw91/6-311+g(2d,p) level. Rotational strengths were predicted on the most stable conformers for 20 excited states at the b3lyp/6-311+g(d,p) level. Cartesian coordinates of the most population are accessible at https://Fig.share.com/s/4e224ec1ec45de75b4f8 (10.6084/m9.Fig.share.9165314). ECD spectra were plotted using GaussView 6. DP4 scores were calculated using the original java script from Goodman's lab.[23]

3. Results and discussion

3.1. Structure elucidation of new compounds (**1**−**4**)

Compounds **1**–**4** were isolated from the acetone extract of *U. baileyi* by successive column chromatography (Fig. 1).

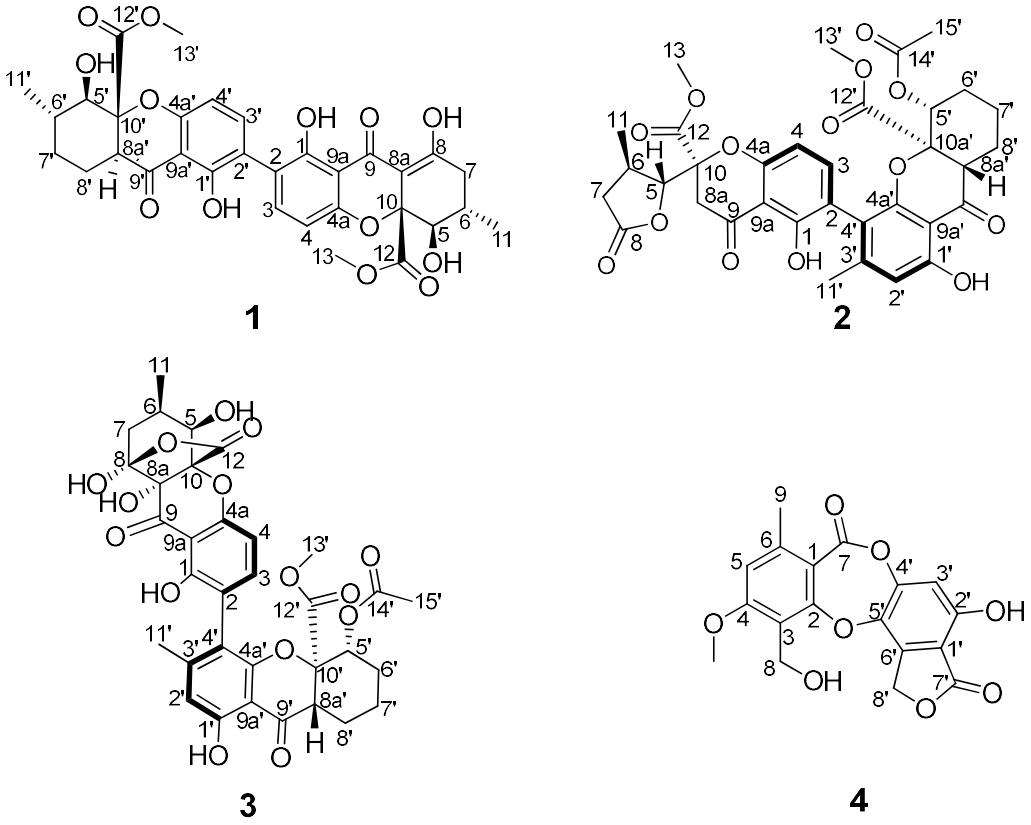

Fig. 1. Structures of compounds **1**–**4**.

The molecular formula of **1** could be established as $C_{32}H_{32}O_{13}$ based on ^{13}C NMR and HRESIMS data, verifying the presence of 18 double-bond equivalents. Owing to molecular formula requirements and 30 protons being evident from ^{1}H NMR analysis, two protons were deduced to occur as aliphatic hydroxy groups. The ^{1}H and HSQC spectrum revealed three hydrogen-bonded hydroxy groups at δ_H 13.77 (1H, s, OH-8), 11.88 (1H, s, OH-1) and 11.73 (1H, s, OH-1′) ; two pairs of *ortho*-oriented aromatic protons at δ_H 7.48 (2H, d, *J* = 8.5 Hz, H-3 and H-3′) and 6.63 (2H, d, *J* = 8.5 Hz, H-4 and H-4′) ; two oxygenated methine signals at δ_H 3.93 (1H, d, *J* = 11.5 Hz, H-5) and 3.73 (1H, d, *J* = 10.5 Hz, H-5′) ; three methine signals at δ_H 2.98 (1H, dd, *J* = 12.0, 4.5 Hz, H-8a′), 2.42 (1H, m, H-6) and 1.83 (1H, m, H-6′) ; three diastereotopic pairs of methylene hydrogens at δ_H 2.74 (1H, dd, *J* = 19.0, 6.0 Hz, H-7) and 2.32 (1H, dd, *J* = 19.0, 10.5 Hz, H-7) ; at δ_H 2.20 and 2.15 (2H, m, H_2-8′) and at δ_H 1.95 (1H, m, H-7′) and 1.21 (1H, m, H-7′) ; two methoxy signals at δ_H 3.70 (3H, s, H_3-13) and at δ_H 3.73 (3H, s, H_3-13′); two methyl groups at δ_H 1.17 (3H, d, *J* = 6.5 Hz, H_3-11) and at 1.12 (3H, d, *J* = 6.5 Hz, H_3-11′). The two methoxy groups could be straightforwardly defined as methyl ester moieties based on HMBC correlations from H_3-13′ to C-12′ and from H_3-13 to C-12. The ^{13}C NMR spectrum of compound **1** revealed an apparent twinning for many carbon resonances, suggesting that it might correspond to a dimeric structure with some slight differences between each subunit. The scaffold of each monomer could be determined to be a xanthone.

A first subunit was determined as a hexahydroxanthone based on the COSY spectrum which allowed the development of a spin system identified as H-5′/H-6′/(H_3-11′)/H_2-7′/H_2-8′/H-8a′. The chemical shift of C-5′ (δ_C 80.3) was indicative of the *ipso* location of a first aliphatic hydroxy group. The C-10′ location of the methyl ester group

could be determined from the long-range heteronuclear correlation from both the oxymethine proton H-5′ at δ_H 3.73 and the oxymethine proton H-8a′ at δ_H 2.98 to C-12′. The chemical shift value of C-10′ indicated that this carbon was oxygenated and the HMBC correlations from H-8′ to C-9′ and from H-8a′ to C-4a′ and C-9a′ defined a chromenone core. A second spin system in this monomer involved two *ortho*-oriented aromatic protons and the connection of this phenyl ring to the γ-pyrone nucleus of the hexahydroxanthone could be deduced from long-range heteronuclear correlations from the aromatic protons H-3′ at δ_H 7.48 and H-4′ at δ_H 6.63 to C-4a′ (δ_C 159.0) and C-9a′ (δ_C 107.4) (Fig. 2). A phenol group could be assigned at C-1′ as evidenced by HMBC correlations from the phenolic proton at δ_H 11.73 to C-1′ (δ_C 159.5), C-2′ (δ_C 118.2) and C-9a′(δ_C 107.4). Due to C-2′ being a quaternary carbon, it can be deemed that this specific site is linked to the other part of the compound.

The second monomer, subunit II, was highly reminiscent of the first one. The most salient spectroscopic difference between the two sub-units being the intense downfield shift of C-8 and C-8a compared to their homologous positions in the first sub-unit (with respective δ_C values of 177.7 and 101.7 vs 20.4 and 51.2 ppm) that indicated the occurrence of an enolic moiety at these positions, as further backed up by the HMBC cross-peaks between the hydrogen-bonded hydroxy group OH-8 at δ_H 13.77 and C-7 (δ_C 36.4), C-8 (δ_C 177.7) and C-8a (δ_C 101.7). NMR signal patterns related to this subunit, including COSY and HMBC data, confirmed a similar gross structure of the rest of this monomer, compared to that of sub-unit I. Due to ^{1}H NMR resonances for two *ortho* oriented aromatic protons, the only remaining possibility for monomeric units linkage was a bond tethering C-2 with C-2′. The steric hindrance generated by the substituents *ortho* to the biaryl junction (two OH and two H) is not sufficient to lead to true atropisomerism.[11, 24]

The absolute configurations of 2,2′-secalonic acids similar to compound **1** could be reliably determined from their n-π* ECD bands around 330 nm, that are correlated with the configuration *S* of the C-10 and C-10′ stereogenic centers.[25, 26] A positive n-π* ECD band (333 nm, Δε = + 12.3) determined (10*R*, 10′*R*) configurations and also allowed the assignment of the other stereogenic centers based on the relative stereochemistry, in excellent agreement with literature data (Fig. 3).[11, 27, 28] Accordingly, the magnitude of the vicinal coupling constant value of the oxymethine proton at H-5/H-5′ bisects the dihedral angle of the adjacent proton(s). Regarding the currently described structure, the elevated coupling constant of H-5 and H-5′ determined the axial position of both these oxymethine protons and established the C-5/C-6 and C-5′/C-6′ trans-diaxial configuration, as in blennolide B or xantholepinone A among others ($^3J_{H\text{-}5,H\text{-}6}$=11.5 Hz and $^3J_{H\text{-}5',H\text{-}6'}$=10.5 Hz).[11, 29] This deduction was further supported by ROESY correlations between the oxymethine proton at δ_H 3.73 (H_3-5′) and both the methyl group at δ_H 1.12 (H_3-11′) and the methine proton at δ_H 2.98 (H-8a′) that determined the synfacial orientation of these substituents. The axial orientation of H-5 was diagnostic of a space arrangement identical to that of eumitrin A2 rather than that of eumitrin A1/eumitrin B[as further ascertained on various bisxanthone scaffolds.[27, 30] The absolute stereostructure assignment of C-5 was at last supported by the comparison of the NMR data of the long sought-after tetrahydroxanthone hemisecanolic acid monomers, blennolide B and its C-5 epimer, blennolide C, jointly determining a 5*R,* 5*R*′ configuration .[11] Thus, the (5*R*, 6*S*, 10*R*, 5′*R*, 6′*S*, 8a′*S*, 10′*R*)-absolute configuration of **1**, namely eumitrin C, was determined as displayed on Fig. 1.

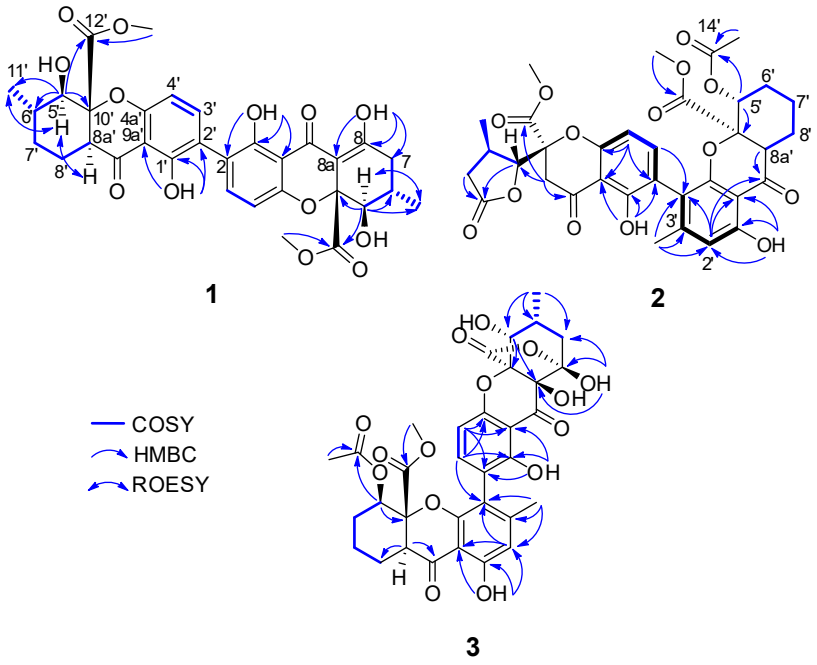

Fig. 2. Key COSY, HMBC and ROESY correlations of compounds **1**–**3**.

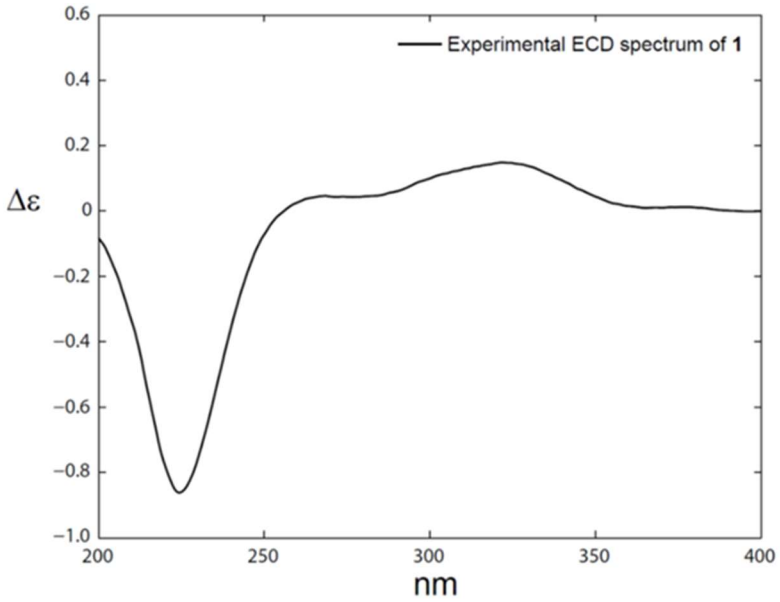

Fig. 3. Experimental ECD spectrum of compound **1**.

Compound **2** was isolated as a light yellow, amorphous solid. Its molecular formula was determined to be $C_{34}H_{34}O_{14}$ based on the sodiated ion peak at *m/z* 689.1820 (calcd for $C_{34}H_{34}O_{14}Na$, 689.1841). In spite of their closely related molecular formulas, the examination of the ^{1}H and ^{13}C NMR spectra revealed some important structural differences with compound **1** including the lack of the enolic signals that indicated the absence of a $\Delta^{8(8a)}$ double bond and the occurrence of an acetoxycarbonyl group that could be located at C-5′ based on the HMBC correlations from the acetoxycarbonyl protons at δ_H 2.00 (H_3-15′) to C-14′ (δ_C 169.8) and C-5′ (δ_C 72.6), as further backed up by the HMBC crosspeak between the oxymethine proton H-5′ (δ_H 5.03) and C-14′. Likewise, one of the methyl groups

was downfield shifted to a value of δ_H 2.13 indicating its aromatic nature, consistently with the disappearance of an aromatic proton signal and with the singlet status of the aromatic proton at δ_H 6.49 (H-2'). This methyl group was indeed located at C-3', based on the long-range heteronuclear correlations from these protons to C-2' (δ_C 111.4), C-3' (δ_C 151.0), and C-4' (δ_C 115.5). The COSY spectrum revealed the H-5'/H_2-6'/H_2-7'/H_2-8'/H-8a' proton spin system, further supported by the full set of possible ^2J and ^3J correlations observed in the HMBC spectrum that established the hexahydroxanthone scaffold of a first monomer. The synfacial orientation of the acetoxycarbonyl and of the methyl ester groups was established from the H_3-13'/H_3-15' ROE crosspeak while the key ROE effect between the oxymethine proton at δ_H 5.03 (H-5') and the methine proton at δ_H 2.97 (H-8a') ascribed these protons to the other face of the structure. As formerly observed for compound **1**, the vicinal coupling constant value of the oxymethine proton H-5' determined its axial orientation and thus defined a 5'*R* configuration identical to that of blennolide B to define the structure of this first subunit as displayed on Fig. 1.

The remaining signals were assigned to a hydrogen-bonded hydroxy proton at δ_H 11.75, *ortho*-oriented aromatic protons at δ_H 6.58 and 7.76, an oxygenated methine proton at δ_H 4.47, an aliphatic methine at δ_H 2.89, a diastereotopic methylene at δ_H 2.32/2.16 and a methyl group at δ_H 1.30. The thorough analysis of long-range heteronuclear correlations established a partially saturated γ-pyrone system annulated to an aromatic ring. The molecular formula of **2** determined a double bond equivalent of 18, and the presence of the pentacyclic biaryl scaffold determined so far along with the five carbonyl carbons [δ_C 175.4 (C-8), 170.3 (C-12'), 169.8 (C-14'), and 168.9 (C-12)] accounted for 17 elements of unsaturation, thereby leaving one aliphatic ring system to be introduced in the remaining part of the molecule. Accordingly, the analysis of the COSY spectrum revealed the proton spin system of H-5/H-6/H_3-11/H-7 which was cyclized to afford a β-methyl-γ-lactone moiety as deduced from HMBC correlations of the oxymethine proton at δ_H 4.47 (H-5), the methine proton at δ_H 2.89 (H-6), and the diastereotopic methylene protons at δ_H 2.24 and 2.95 (H_2-7) to C-8 (δ_C 175.4). The key HMBC correlations from the methylene protons H_2-8a to C-5 (δ_C 87.7), C-9 (δ_C 194.4), C-10a (δ_C 84.6) and C-12 (δ_C 168.9) defined the connection between the chromone core and both the γ-butyrolactone moiety and the ester group, as depicted in Fig. 1. The planar structure of **2** was obtained by connecting the two monomeric units *via* the linkage of hexahydroxanthone C-4' and chromanone C-2, evidenced by the HMBC correlation of the aromatic proton at δ_H 7.76 (H-3) to C-4' (δ_C 115.5) and from the aromatic methyl protons at δ_H 2.13 to C-4'. The oxymethine proton H-5 was coupled to the tertiary methine proton H-6 with a coupling constant of 3.5 Hz, characteristic of *trans*-oriented protons in such ring system[31], as further validated by ROE correlation between H-5 and CH_3-11. The strong ROE correlation between the oxymethine proton H-5 and both the diastereotopic methylene protons H-8a indicated the pseudoequatorial position of this substituent. This deduction was supported by the interunit H-3/H-11' ROE crosspeak, as earlier reported on dimeric tetrahydroxanthone neosartorin that displays the same relative configuration and axial chirality.[32]

The structure of **2** comprised a rotationally hindered biaryl axis, as evidenced by the axial chirality of compounds being similarly *ortho*-substituted to the stereogenic biaryl axis.[12, 32] Each monomer of compound **2** revealed a benzoyl chromophore with a maximum UV absorption near 240 nm. Based on the blennolide series, it was demonstrated that the ECD Cotton effects at this wavelength did not split.[11] On the opposite, the axially linked dimers display obviously split CE indicating that the chromophores interacted with each other, as revealed by their opposite but not mirror ECD spectra plots. In such structures, axial chiralities governed chromophore spatial position and the ECD spectrum.[12, 33-35] Thus, the chromophores' rotary manners were identical to those of the CD Exciton Chirality Rule. The anticlockwise manner of the two benzoyl chromophores of compound **2** could be deduced from the negative exciton couplet centered at around 240 nm ; consistently with earlier reports on related structures,[12, 32] as further backed up by the ROE correlation between H-3 and H_3-11' (Fig. 4). The absolute

configuration of the γ-butyrolactone ring was deduced by comparison between both predicted spectra with the experimental one, which revealed an excellent fit for a (a*S*, 5'*R*, 8a'*R*, 10'*R*, 5*R*, 6*R*, 10*S*) configuration (Fig. 5).

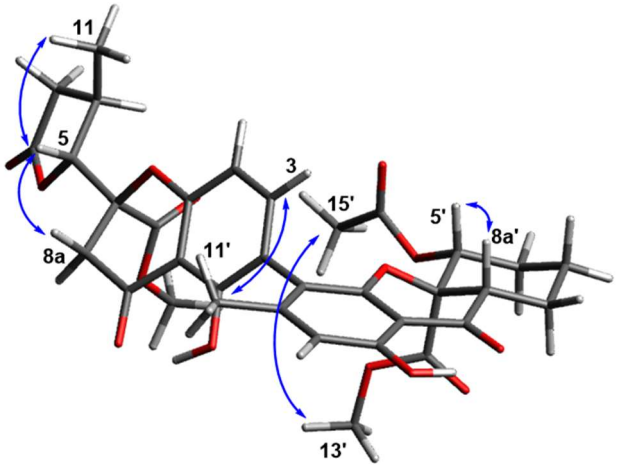

Fig. 4. Key ROE correlations of compound **2**.

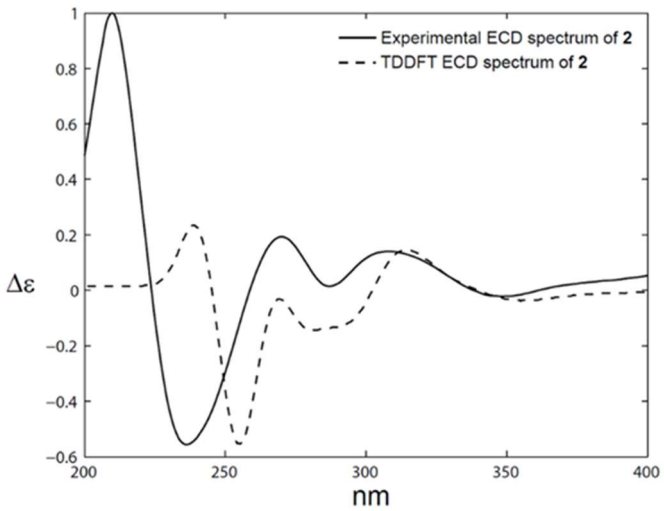

Fig. 5. Comparison of the experimental ECD spectrum of **2** and calculated ECD spectrum for the (a*S*, 5'*R*, 8a'*R*, 10'*R*, 5*R*, 6*R*, 10*S*) stereoisomer (UV shift = - 12 nm).

Compound **3** was obtained as a light yellow, amorphous solid. Its molecular formula was determined as $C_{33}H_{32}O_{15}$ based on HRESIMS measurements (*m/z* 667.1658 calcd for 667.1668 $[M-H]^-$) and ^{13}C NMR data. The ^1H NMR spectrum showed 30 protons, revealing the occurrence of 2 supplementary aliphatic hydroxyl groups. The thorough analysis of the 2D NMR spectra determined a similar hexahydroxanthone monomeric building unit as in compound **2**. As to the other subunit, the occurrence of a hydrogen-bonded hydroxy proton at δ_H 11.30 and the *ortho*-oriented aromatic protons at δ_H 7.85 and 6.69 determined the unchanged constitutions of A and B rings, as further supported by the key long-range heteronuclear correlations outlined in Fig. 2. The structural features elucidated so far account for 15 indices of hydrogen deficiency, leaving three more to be introduced, while five more oxygen atoms still have to be incorporated into the structure. The COSY spectrum revealed the H-5/H-6/(H_3-11)/H_2-7 spin system, along with the HMBC correlations from the methyl protons at δ_H 1.22 to C-5 (δ_C 74.8), C-6 (δ_C 29.8), and C-7 (δ_C 34.0). An

aliphatic hydroxyl group could be located at C-8 based on the long-range heteronuclear correlations from the hydroxyl proton at δ_H 7.09 to C-7, C-8 (δ_C 108.9), and C-8a (δ_C 73.6). The linkage of the OH group to the carbon resonating at δ_C 108.9 was determined based on the HMBC cross-peak between the oxymethine proton at δ_H 4.37 and C-8a. Owing to molecular formula requirements and to connectivity constraints, a bicyclic framework tethering C-8a with C-10 through a lactone could be determined, which was consistent with the resonating of C-8 at δ_C 108.9 that is itself indicative of an hemiketalic carbon. Likewise, the chemical shift of the tertiary carbon at δ_C 84.6 is in excellent agreement with earlier reports on molecules bearing a methyl ester group at this specific position.[11, 12, 30] Similar to **2**, the a*S* axial chirality of **3** could be determined based on the negative exciton couplet at 240 nm.[10] The (10*R*/10'*R*) absolute configuration s could be determined based on the positive sign of the band *ca.* 330 nm Δε = +9). The validity of using this band to assign the absolute configuration s of these stereogenic centers was demonstrated on both ester/ester (e. g secalonic acid B), lactone/ester (e. g ergochrysine B), and lactone/lactone (e. g ergoflavine) xanthone dimers.[36] The null coupling constant value between H-5 and H-6 indicated their synfacial orientation,[11, 37] as further validated by the ROE crosspeak between H-5 and H-6. This relative stereochemistry is in excellent agreement with ^{13}C NMR spectroscopic data of usneaxanthones A–C[10]. Information regarding the relative stereochemistry of this subunit were also completed by the ROE correlation between both the hydroxyl at δ_H 6.38 (8a-OH) and at 7.09 (8-OH) and the oxygenated methine at δ_H 4.37 (H-5), ascribing these substituents to the same side of the cyclohexane nucleus. The relative stereochemistry of the lactone moiety could not be assigned based solely on spectrum. The comparison of the ^{13}C NMR data of the two candidate diastereoisomers with the observed chemical shifts of **3** through Goodman and Smith DP4 parameter resulted in the prediction of the relative configuration with a 92.7% probability (Fig. 6). This determined stereochemistry was further validated by the excellent agreement between the ECD plot of **3** with that of the recently reported usneaxanthone A, the absolute stereochemistry of which was unambiguously determined through single crystal X-ray diffraction analysis (Fig. 7). The substitution patterns of the monomeric units being reported herein are indicative of their originating from chrysophanol, following the so-called ravenelin pathway that leads to xanthones displaying a methyl group at C-3.[2] The understanding of the underlying biosynthetic pathways giving rise to xanthone dimers dramatically rose through a series of gene-deletion experiments carried out in the neosartorin-producing fungus *Aspergillus novofumigatus*.[38] The biosynthesis of the monomeric building blocks was proved to proceed from chrysophanol *via* a Baeyer-Villiger monooxygenase, a methyltransferase, a reductase and an acetyltransferase. The heterodimerization would then involve a p450 monooxygenase that most interestingly revealed sequence similarity with a p450 encoded upstream of the biosynthetic gene cluster of ergochrome xanthone dimers within *Claviceps purpurea*.[39] Despite being related to xanthone dimers being formerly reported to occur throughout literature, the newly described compounds display rather uncommon structural features. At first, eumitrin C stands among the rare tetrahydroxanthone/hexahydroxanthone dimers, a scaffold only being sustained so far by ergochromes AD and BD,[40] and eumitrins A_2 and B.[3] Xanthone monomers were already related to 2,2-disubstituted chroman-4-ones, particularly in fungi.[6, 41] The γ-butyrolactone ring of such chromanones results from a retro-Dieckmann cyclization, sometimes being accompanied by further ring cleavage intermediates such as the related γ-hydroxybutyric acid derivatives and their corresponding methyl esters.[12, 30] Although being biogenetically related, xanthone/chromanone heterodimers are rare, being so far represented by related cases comprising blennolide G,[11, 42] blennolides I and J,[43] gonytolides D and E,[12] phomolactonexanthones,[44] and versixanthones A–F.[30] As far as can be ascertained, eumitrin D represents the first occurrence of xanthone dimer comprising a hexahydroxanthone and a chromanone. Lactone-comprising xanthone dimers were scarcely reported throughout literature with 5 such compounds initially found within this structural class, first as ergot pigments: the lactone/lactone ergoflavin[45] and the lactone/ester-based ergochrysins A and B,[40] ergochrome CD,[46] and ergoxanthin.[47, 48] A suite of lactone/ester bisxanthones, *viz.* usneaxanthones A–C from *Usnea aciculifera*, very recently extended the number of compounds

from this structural class, the structure elucidation of which was greatly aided by them having crystallized.[10] The lactonic monomer of **3** is unique due to C-8 hydroxylation that introduces an unprecedented hemiketalic function. Although unprecedented, the 8-OH group of the lactonic monomer of eumitrin E is also in line with the canonical substitution pattern of ravenelin-derived xanthones.[49] The 2-4′ biaryl linkage is shared with usneaxanthones but not with lactone/ester xanthone heterodimers which was not reported so far within lactone/ester based xanthone dimers. These newly reported structures may correspond to the sought-after eumitrins A3 and B2, reported from *U. baileyi* as well, that were named but not yet structurally elucidated, or also to either eumitrin U, X or Y. Nevertheless, since the authors cannot prove that these metabolites match any of these formerly described compounds, it was decided to name the new dimers xanthones with unprecedented designations.

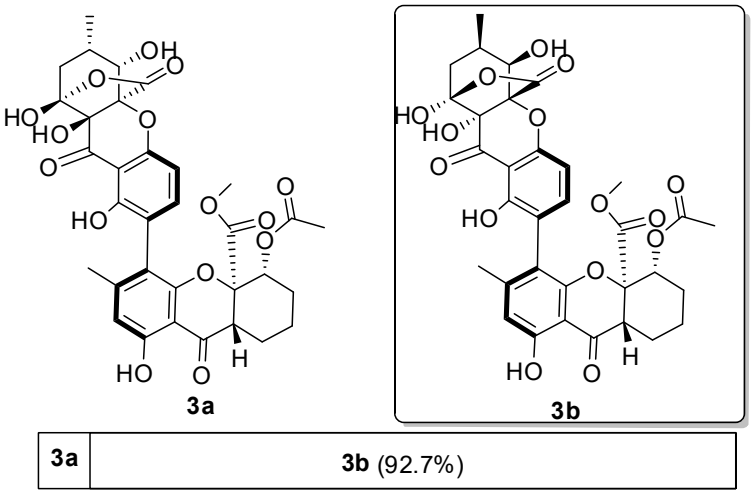

Fig. 6. Relative configuration for Eumitrin E (**3**): DP4 probabilities of the two candidate diastereoisomers.

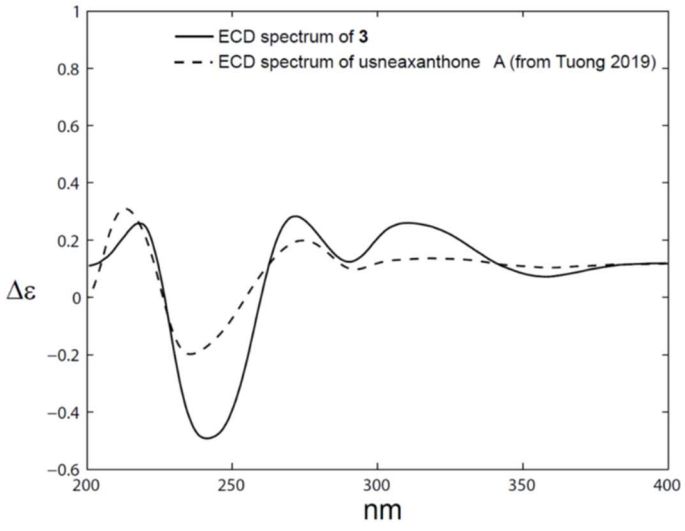

Fig. 7. Comparison of the experimental ECD spectrum of **3** and usneaxanthone A [reproduced with permission from[10]].

Table 1
^{1}H (500 MHz) and ^{13}C (125 MHz) NMR Data for **1**−**3** ($CDCl_3$).

	Eumitrin C (**1**)		Eumitrin D (**2**)		Eumitrin E (**3**)	
No.	δ_H	δ_C	δ_H	δ_C	δ_H	δ_C
1		159.0		159.5		161.4
2		117.7		107.5		118.5
3	7.48 d (8.5)	140.4	7.76 d (8.5)	143.1	7.85 d (8.5)	145.4
4	6.63 d (8.5)	107.7	6.58 d (8.5)	107.3	6.69 d (8.5)	107.5
4a		158.4		159.0		158.3
5	3.93 d (11.5)	77.1	4.47 d (3.5)	87.7	4.37 s	74.8
6	2.42 m	29.4	2.89, 1H, m	30.1	2.16 m	29.8
7	2.74 dd (19.0, 6.0) 2.32 dd, (19.0, 10.5)	36.4	2.95 dd (17.0, 8.5) 2.24 dd (17.5, 4.0)	36.3	2.35 m 2.16 m	34.2
8		177.7		175.4		108.9
8a		101.7	3.22 d (17.0) 3.10 d (17.0)	39.9		73.6
9		187.3		194.4		195.0
9a		107.3		117.3		106.7
10a		84.9		84.6		84.6
11	1.17 d (6.5)	18.1	1.30 d (7.0)	21.0	1.22 d (6.0)	15.1
12		169.3		168.9		165.5
13	3.70 s	53.0	3.67 s	53.4		
14						
15						
1-OH	11.88 s		11.75 s		11.30 s	
8-OH	13.77 s				7.09 br s	
8a-OH					6.38 br s	
1′		159.5		161.8		162.0
2′		118.2	6.49 s	111.4	6.50 s	111.4
3′	7.48 d (8.5)	140.4		151.0		150.7
4′	6.63 d (8.5)	107.7		115.5		115.0
4a′		159.0		156.5		156.7
5′	3.73 d (10.5)	80.3	5.03 dd (12.0, 5.0)	72.6	5.01 dd (12.0, 5.0)	72.6
6′	1.83 m	34.3	1.66 m 1.74 m	26.1	1.80 m 1.69 m	26.3
7′	1.95 m 1.21 m	31.2	1.86 m 1.52 m	22.4	1.89 m 1.52 m	22.4
8′	2.15 - 2.20 m	20.4	1.86 m 1.52 m	25.3	1.89 m 1.52 m	25.6
8a′	2.98 dd (12.0, 4.5)	51.2	2.97 dd (12.0, 5.0)	48.7	2.97 dd (12.5, 4.5)	48.8
9′		197.4		197.6		197.6
9a′		107.4		104.9		104.9
10′		87.5		83.4		83.6
11′	1.12 d (6.5)	18.4	2.13 s	21.2	2.13 s	21.9
12′		170.4		170.3		169.8
13′	3.73 s	53.4	3.71 s	53.4	3.66 s	53.4
14′				169.8		170.4
15′			2.00 s	20.9	1.94 s	20.8
1′-OH	11.73 s		11.47 s		11.48 s	

Compound **4** was isolated as a white amorphous solid and was assigned the molecular formula $C_{18}H_{14}O_8$ (12 indices of hydrogen deficiency) based on its negative-ion HRESIMS data which showed an $[M-H]^-$ peak at *m/z* 357.0614 (calcd. for $C_{18}H_{13}O_8$, 357.0616). The ^1H NMR data revealed typical resonances of an aromatic methyl at δ_H 2.52 (3H, s), a methoxy group at δ_H 3.94 (3H, s), two oxygenated methylene [(δ_H 4.81, 2H, s) and (δ_H 5.69, 2H, s)],

and two aromatic protons at δ_H 6.68 (1H, s) and at δ_H 6.81 (1H, s). The small amount of **4** precluded the acquisition of a ^{13}C NMR spectrum of sufficient quality, but all of the chemical shifts could be deduced from inverse-detection heteronuclear NMR spectra (Table 2).

The β-orcinol depsidone scaffold was deduced by the near-identical 1D NMR data of **4** with those of cryptostictinolide, as reported by Lohézic-Le Dévéhat *et al*. from *Usnea articulata*,[50] and further backed up by 2D NMR correlations (Fig. 8). The chemical shift value of C-3′ (δ_C 108.8) is diagnostic of it being *ortho*-oriented to two oxygen functions, identifying **4** as 3′-*O*-demethylcryptostictinolide, also evidenced by the HMBC correlations from the aromatic proton at δ_H 6.81 to C-1′ (δ_C 107.5), C-2′ (δ_C 151.6), C-4′ (δ_C 151.7), and C-5′ (δ_C 138.3) (Fig. 8).

Table 2
^1H (500 MHz) and ^{13}C (125 MHz) NMR Data for **4** ($CDCl_3$).

No.	δ_H	δ_C
1		113.7
2		158.5
3		117.2
4		160.8
5	6.68 s	111.1
6		145.6
7		nd
8	2.52 s	21.7
9	4.81 s	53.8
4-OMe	3.94 s	56.4
1′		107.5
2′		151.6
3′	6.81 s	108.8
4′		151.7
5′		138.3
6′		138.3
7′		171.9
8′	5.69 s	68.7

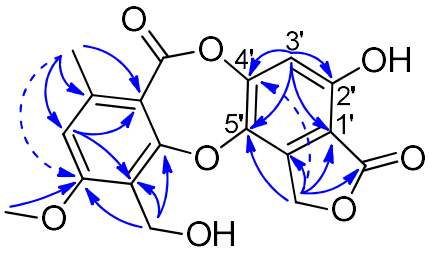

Fig. 8. Key HMBC correlations of compound **4**.

3.2. Biological Testing of Xanthone Dimers 1−3**.**

The purified xanthone dimers **1**–**3** were evaluated in vitro for their antiparasitic activity against the chloroquine-resistant strain of *Plasmodium falciparum* FcB1 as well as for the cytotoxic activity against a panel of 7 representative cell lines, as indicated in Table 3. Bisxanthones **1**–**3** revealed weak (compounds **1**–**2**) or no (compound **3**) antiparasitic activity (Table 3). As to cytotoxicity assays, only compound **2** exerted a moderate effect

against the tested cell lines (Table 3).MCF-7 cell line resulted slightly more susceptible with an IC_{50} value of 12 µM. Even though some xanthone dimers, such as the well-known phomoxanthone A,[8] were associated with significant cytotoxicity against a variety of cell lines, bisxanthones comprising a γ- butyrolactone-related chromanone and a xanthone subunit tethered with either a 2,4′- or a 4,2′-linkage were reported to exhibit quite selective cytotoxicity in some cases with low-micromolar IC50 values[30] while in other cases showed no activity on the assayed cells.[44]

Table 3

IC_{50} values (µM) of the Antiplasmodial, and Cytotoxic Activities of Compounds **1**–**3**.

Compound	*P. falciparum* strain FcB1	HuH7	Caco-2	MDA-MB-231	HCT116	PC3	MDA-MB-468	MCF7	Fibroblasts
1	96.5 ± 3.5	> 50	> 50	> 50	> 50	> 50	> 50	> 50	> 50
2	73.0 ± 1.0	35	44	> 50	> 50	42	> 50	12	> 50
3	>100	> 50	> 50	> 50	> 50	> 50	> 50	> 50	> 50
Chloroquine	0.05 ± 0.02	-	-	-	-	-	-	-	-
Roscovitine	-	12.5	17	17	9	11	16	10	> 50
Paclitaxel	-	0.01	0.04	0.02	0.01	0.01	0.01	0.01	> 50
Doxorubicin	-	0.06	0.05	0.03	0.08	0.04	0.04	0.08	> 50

4. Conclusions

In conclusion, we have conducted the successful isolation and structure elucidation of four new compounds, including three xanthone dimers eumitrins C–E (1–3) and a new depsidone, 3′-O-demethylcryptostictinolide (4), from the vietnamese fruticose lichen Usnea baileyi. The structure elucidation of the three bisxanthones (1–3) was highly challenging owing to their elevated number of asymmetric carbons (7, 6, and 8, respectively), along with a stereogenic biaryl axis for these last two compounds. Accordingly, these substances benefitted from an extensive set of spectroscopic analyses including HRMS, NMR, and ECD. The absolute configuration of 2 was ascertained by comparison to TDDFT calculations while the stereochemistry of 3 benefitted from DFT-NMR calculations of the two remaining diastereoisomeric candidates and subsequent DP4 probability score. This eumitrin series stand among the very few xanthone dimers to be fully elucidated without the support of single-crystal X-ray diffraction analysis.

*Eumitrin C (**1**):* yellow, amorphous solid. $[\alpha]^{20}_{D}$ + 28.00 (c 0.02, MeOH) ; λ_{max} (log ε) 205 (4.2), 249 (3.2), 339 (4.1) nm ; IR (KBr) ν_{max} 3400, 2907, 1732, 1628, 1424, 1335, 1258, 1212 cm^{-1} ; HRESIMS *m/z* 623.1792 $[M-H]^-$ (calcd. for $C_{32}H_{31}O_{13}$, 623.1770). ^1H and ^{13}C NMR ($CDCl_3$) see Table 1.

*Eumitrin D (**2**):* yellow, amorphous solid. $[\alpha]^{20}_{D}$ - 114.70 (c 0.02, MeOH) ; λ_{max} (log ε) 205 (3.1), 278 (1.6), 336 (1.4) nm; IR (KBr) ν_{max} 3455, 2959, 1746, 1628, 1453, 1368, 1218 cm^{-1} ; HRESIMS *m/z* 689.1820 $[M+Na]^+$ (calcd. for $C_{32}H_{32}O_{13}Na$, 689.1841). ^1H and ^{13}C NMR ($CDCl_3$) see Table 1.

*Eumitrin E (**3**):* yellow, amorphous solid. $[\alpha]^{20}_{D}$ - 57.00 (c 0.02, MeOH) ; λ_{max} (log ε) 238 (2.7), 270 (1.2), 317 (0.9) nm ; IR (KBr) ν_{max}: 3421, 3379, 1733, 1618, 1304 cm^{-1}; HRESIMS *m/z* 667.1658 $[M-H]^-$ (calcd. for $C_{33}H_{31}O_{15}$, 605.16590). ^1H and ^{13}C NMR ($CDCl_3$) see Table 1.

*3'-O-demethylcryptostictinolide (**4**):* white, amorphous solid. λ_{max} (log ε) 253 (1.9), 306 (2.1) ; IR (KBr) ν_{max}: 3424, 3291, 2951, 1749, 1736, 1729 cm^{-1}; HRESIMS *m/z* 357.0614 $[M-H]^-$ (calcd. for $C_{18}H_{13}O_8$, 357.0616). ^1H and ^{13}C NMR ($CDCl_3$) see Table 2.

Conflicts of interest

There are no conflicts to declare.

Acknowledgements

This work was financially supported by the schorlaship from the Graduate School, Chulalongkorn University to commemorate The 100th Anniversary Chulalongkorn University, the 90th Anniversary Chulalongkorn University Fund (Ratchadaphiseksomphot Endowment Fund) and the Overseas Research Experience Scholarship for Graduate Student. The authors would like to thank N. Dangphui for the authentification of the lichen material. The authors are also indebted to Dr. R. Le Guével (Impaccell) for performing the in vitro tests of cell proliferation inhibition. At last, the authors acknowledge the PRISM platform (Université de Rennes 1) for ECD measurements.

Notes and references

1. J. Boustie and M. Grube, *Plant Genetic Resources*, 2005, **3**, 273-287.
2. P. Le Pogam and J. Boustie, *Molecules*, 2016, **21**, 294.
3. D.-M. Yang, N. Takeda, Y. Iitaka, V. Sankawa and S. Shibata, *Tetrahedron*, 1973, **29**, 519-528.
4. I. Yosioka, T. Nakanishi, S. Izumi and I. Kitagawa, *Chemical and Pharmaceutical Bulletin*, 1968, **16**, 2090-2091.
5. M. Millot, S. Tomasi, E. Studzinska, I. Rouaud and J. Boustie, *Journal of natural products*, 2009, **72**, 2177-2180.
6. T. Wezeman, S. Bräse and K.-S. Masters, *Natural Product Reports*, 2015, **32**, 6-28.
7. T. Qin and J. A. Porco Jr, *Angewandte Chemie International Edition*, 2014, **53**, 3107-3110.
8. M. Frank, H. Niemann, P. Böhler, B. Stork, S. Wesselborg, W. Lin and P. Proksch, *Current medicinal chemistry*, 2015, **22**, 3523-3532.
9. K. C. Ehrlich, L. Lee, A. Ciegler and M. Palmgren, *Appl. Environ. Microbiol.*, 1982, **44**, 1007-1008.
10. T. L. Tuong, T. Aree, L. T. Do, P. K. Nguyen, P. Wonganan and W. Chavasiri, *Fitoterapia*, 2019, **137**, 104194.
11. W. Zhang, K. Krohn, U. Flörke, G. Pescitelli, L. Di Bari, S. Antus, T. Kurtán, J. Rheinheimer, S. Draeger and B. Schulz, *Chemistry–A European Journal*, 2008, **14**, 4913-4923.
12. T.-X. Li, M.-H. Yang, Y. Wang, X.-B. Wang, J. Luo, J.-G. Luo and L.-Y. Kong, *Scientific Reports*, 2016, **6**, 38958.
13. M. Nuno, *Journal of Japanese botany*, 1971.
14. Y. Asahina, *Jour Jap Bot*, 1967, **42**, 1-9.
15. L. B. Din, Z. Zakaria, M. W. Samsudin and J. A. Elix, *Sains Malaysiana*, 2010, **39**, 901-908.
16. F. Bungartz, J. A. Elix and T. H. Nash III, *Bryologist*, 2004, 459-479.
17. M. Giralt, *The Lichenologist*, 2010, **42**, 763-765.
18. J. C. Lendemer, J. W. Sheard, T. Göran and T. Tønsberg, *The Lichenologist*, 2012, **44**, 179-187.
19. K. Van Nguyen, T.-H. Duong, K. P. P. Nguyen, E. Sangvichien, P. Wonganan and W. Chavasiri, *Tetrahedron Letters*, 2018, **59**, 1348-1351.

20. W. K. Coulibaly, L. Paquin, A. Bénie, Y.-A. Békro, R. Le Guével, M. Ravache, A. Corlu and J. P. Bazureau, *Medicinal Chemistry Research*, 2015, **24**, 1653-1661.
21. E. Otogo N'Nang, G. Bernadat, E. Mouray, B. Kumulungui, P. Grellier, E. Poupon, P. Champy and M. A. Beniddir, *Organic Letters*, 2018, **20**, 6596-6600.
22. M. Frisch, G. Trucks, H. Schlegel, G. Scuseria, M. Robb, J. Cheeseman, G. Scalmani, V. Barone, G. Petersson and H. Nakatsuji, *Inc., Wallingford CT*, 2016.
23. S. G. Smith and J. M. Goodman, *Journal of the American Chemical Society*, 2010, **132**, 12946-12959.
24. E. L. Eliel and S. H. Wilen, *Stereochemistry of organic compounds*, John Wiley & Sons, 2008.
25. P. Steyn, *Tetrahedron*, 1970, **26**, 51-57.
26. R. Andersen, G. Buechi, B. Kobbe and A. L. Demain, *The Journal of organic chemistry*, 1977, **42**, 352-353.
27. B. Franck, E. M. Gottschalk, U. Ohnsorge and F. Hüper, *Chemische Berichte*, 1966, **99**, 3842-3862.
28. H. Yamazaki, K. Ukai and M. Namikoshi, *Tetrahedron Letters*, 2016, **57**, 732-735.
29. J. A. Elix, L. Liao and R. A. Barrow, *Australas. Lichenol*, 2019, **84**, 3-9.
30. G. Wu, G. Yu, T. Kurtan, A. Mandi, J. Peng, X. Mo, M. Liu, H. Li, X. Sun and J. Li, *Journal of natural products*, 2015, **78**, 2691-2698.
31. J. G. Napolitano, J. A. Gavín, C. García, M. Norte, J. J. Fernández and A. Hernández Daranas, *Chemistry–A European Journal*, 2011, **17**, 6338-6347.
32. A. R. B. Ola, A. Debbab, A. H. Aly, A. Mandi, I. Zerfass, A. Hamacher, M. U. Kassack, H. Brötz-Oesterhelt, T. Kurtan and P. Proksch, *Tetrahedron Letters*, 2014, **55**, 1020-1023.
33. H.-J. Zhang, Y.-M. Zhang, J.-G. Luo, J. Luo and L.-Y. Kong, *Organic & Biomolecular Chemistry*, 2015, **13**, 7452-7458.
34. B. Elsässer, K. Krohn, U. Flörke, N. Root, H. J. Aust, S. Draeger, B. Schulz, S. Antus and T. Kurtán, *European journal of organic chemistry*, 2005, **2005**, 4563-4570.
35. N. Harada and K. Nakanishi, *Accounts of Chemical Research*, 1972, **5**, 257-263.
36. B. Franck and G. Baumann, *Chemische Berichte*, 1966, **99**, 3863-3874.
37. A. J. Szwalbe, K. Williams, Z. Song, K. de Mattos-Shipley, Jason L. Vincent, A. M. Bailey, C. L. Willis, R. J. Cox and T. J. Simpson, *Chemical Science*, 2019, **10**, 233-238.
38. Y. Matsuda, C. H. Gotfredsen and T. O. Larsen, *Organic Letters*, 2018, **20**, 7197-7200.
39. L. Neubauer, J. Dopstadt, H.-U. Humpf and P. Tudzynski, *Fungal Biology and Biotechnology*, 2016, **3**, 2.
40. B. Franck and G. Baumann, *Chemische Berichte*, 1966, **99**, 3875-3883.
41. K.-S. Masters and S. Bräse, *Chemical Reviews*, 2012, **112**, 3717-3776.
42. S. Cai, J. B. King, L. Du, D. R. Powell and R. H. Cichewicz, *Journal of Natural Products*, 2014, **77**, 2280-2287.
43. T. El-Elimat, M. Figueroa, H. A. Raja, T. N. Graf, S. M. Swanson, J. O. Falkinham III, M. C. Wani, C. J. Pearce and N. H. Oberlies, *European Journal of Organic Chemistry*, 2015, **2015**, 109-121.
44. B. Ding, J. Yuan, X. Huang, W. Wen, X. Zhu, Y. Liu, H. Li, Y. Lu, L. He, H. Tan and Z. She, *Marine Drugs*, 2013, **11**, 4961-4972.
45. A. T. McPhail, G. A. Sim, J. D. M. Asher, J. M. Robertson and J. V. Silverton, *Journal of the Chemical Society B: Physical Organic*, **1966**, 18-30.
46. B. Franck, *Angewandte Chemie International Edition in English*, 1969, **8**, 251-260.
47. D. J. Aberhart and P. de Mayo, *Tetrahedron*, 1966, **22**, 2359-2366.
48. J. W. Hooper, W. Marlow, W. B. Whalley, A. D. Borthwick and R. Bowden, *Journal of the Chemical Society C: Organic*, **1971**, 3580-3590.
49. J. G. Hill, T. T. Nakashima and J. C. Vederas, *Journal of the American Chemical Society*, 1982, **104**, 1745-1748.
50. F. Lohézic-Le Dévéhat, S. Tomasi, J. A. Elix, A. Bernard, I. Rouaud, P. Uriac and J. Boustie, *Journal of Natural Products*, 2007, **70**, 1218-1220.